Measurements of out-of-plane dynamics induced in magnetic nanopillars by spin transfer

Weng Lee Lim, Andrew Higgins, and Sergei Urazhdin
Department of Physics, West Virginia University, Morgantown, West Virginia 26506, USA
(Received 23 April 2009; revised manuscript received 23 June 2009; published 11 September 2009)

Electrical current can induce very large amplitude of precession in nanomagnets, resulting in highly nonlinear dynamical regimes unattainable by any other means of excitation. We performed spectroscopic measurements of magnetic nanodevices whose geometry was optimized for coherent dynamics at high currents. The dependence of the observed spectroscopic features on the direction of the magnetic field is consistent with the out-of-plane precessional mode, as confirmed by micromagnetic simulations. The dynamics are asymmetric with respect to the inversion of the field, which is highly unusual for magnetic phenomena not involving exchange bias. Micromagnetic simulations indicate that the asymmetry is likely caused by a combination of the Oersted field generated by the current and sample shape imperfections.

DOI: 10.1103/PhysRevB.80.104408 PACS number(s): 75.60.Jk, 75.70.Cn, 85.75.−d

I. INTRODUCTION

Spin-transfer torque (ST) (Ref. 1) exerted on nanomagnets by spin-polarized current I can induce dynamical states not accessible by any other techniques, providing a unique opportunity to test our understanding of nanomagnetism. Simulations show that at I just above excitation threshold, ST causes elliptical precession of the magnetic moment $\mathbf{m}_1$ of a nanomagnet F_1. The precession orbit is determined by a combination of the magnetic field $\mathbf{H}$ and the anisotropy of F_1.[2–4] The latter is usually a thin film whose anisotropy is dominated by its demagnetizing field, with $\mathbf{H}$ commonly in the film plane. The precession amplitude grows with I, resulting in an orbit known as the clamshell mode (inset in Fig. 2). This mode has been extensively measured.[5,6]

Simulations of current-induced dynamics[2–4] suggest that the extreme points of the clamshell can merge at large I, resulting in a crossover to the out-of-plane (OP) precession mode consisting of either the lower or the upper half of the clamshell. The OP mode can be distinguished from other dynamical states by several expected spectroscopic features. First, the frequency of the OP mode is approximately twice the frequency of clamshell near the crossover since its trajectory is half of clamshell. For the same reason, the OP mode should produce microwave signal of amplitude similar to that of clamshell precession. Macrospin simulations indicate that the frequency of the OP mode should increase with I (blueshift),[5] although inhomogeneities can also result in redshifting.[4] In contrast, the clamshell always redshifts with increasing I. Finally, the OP trajectory is highly asymmetric with respect to the sample plane. Therefore, the response of the OP dynamics to out-of-plane tilting of $\mathbf{H}$ should depend on the tilting direction.

A broad large-amplitude spectral feature was previously seen at high I (Ref. 6) but its frequency relationship with clamshell or dependence on the direction of $\mathbf{H}$ were not established. Another feature attributed to the OP mode also did not exhibit the expected frequency relationship with the clamshell precession and its amplitude was two orders of magnitude smaller than expected.[7] The lack of definite observations of high-current spectral feature consistent with the OP mode suggests that simulations may not be adequate for the highly excited dynamical states of nanomagnets or that current-induced effects may not be fully described by the established ST mechanisms.

In sufficiently large nanopillars, the OP precession can be suppressed by spin waves with lower frequency than the OP precession. Additionally, precession can be suppressed by the effect of ST on the polarizing magnetic layer F_2,[8–10] which in the majority of the published spectroscopic measurements had the same lateral dimensions as F_1. Here, we report observation of the OP mode in devices where the latter effect was minimized by using an extended F_2. We analyzed the effects of varied direction of $\mathbf{H}$ and its magnitude H, and verified the expected characteristic features of the OP mode. We also report and discuss the possible mechanisms of the dynamical asymmetry with respect to reversal of $\mathbf{H}$ exhibited by our devices.

II. FABRICATION AND CHARACTERIZATION

Multilayers with structure Cu(50)Py(20)Cu(5) Py(5)Au(20), where Py=$Ni_{80}Fe_{20}$ and thicknesses are in nm, were deposited on oxidized silicon at room temperature (RT) by magnetron sputtering at base pressure of 5×10^{-9} Torr, in 5 mTorr of purified Ar. We patterned F_1=Py(5) and about 5-nm-thick part of F_2=Py(20) by Ar-ion milling through an Al mask with dimensions of 100 nm$\times$50 nm. Oxidation of magnetic nanopillars can significantly affect their current-induced behaviors.[11] To protect our nanopillars from oxidation, we deposited 30 nm of undoped Si immediately after nanopillar patterning, without breaking the vacuum, followed by deposition of a 200-nm-thick Cu top contact. Analysis of the temperature dependence of current-induced behaviors in nanopillars fabricated with our procedure confirms its effectiveness in preventing oxidation.[12]

All measurements were performed at RT. The samples were contacted by coaxial microwave probes connected through a bias tee to a current source, a lock-in amplifier, and a spectrum analyzer through a broadband amplifier. $\mathbf{H}$ was rotated in the sample plane by a finite angle ϕ with respect to the nanopillar easy axis, which is necessary for the spectroscopic detection of odd precession harmonics.[5] Thadani *et al.*[13] as well as the results discussed below show that the

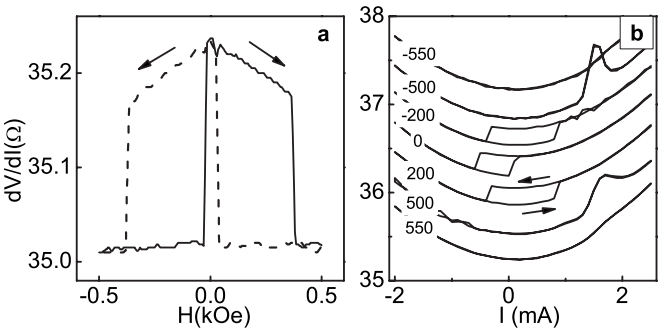

FIG. 1. dc magnetoelectronic properties of the nanopillar, for in-plane **H** rotated in the sample plane by $\phi=40°$ with respect to the nanopillar easy axis. (a) dV/dI vs H and (b) dV/dI vs I, at the values of H as labeled in Oersted. Curves are offset for clarity. Arrows mark the scan direction.

precession coherence is enhanced as ϕ is increased. We performed measurements at $\phi=40°$, unless specified otherwise, which is consistent with the majority of the published spectroscopic measurements. Positive I flowed upward. The measured microwave signals were adjusted for the frequency-dependent gain of the amplifier and losses in the cables and probes, determined with a calibrated microwave generator and a power meter. We report results for one of three tested devices exhibiting similar dynamical features.

Characterization by magnetoresistive (MR) measurements of device response to **H** and I [Fig. 1(a)] yielded MR of 0.21 Ω, which is one of the largest reported RT values for metallic nanopillars. The coercivity of 175 Oe was consistent with monodomain Stoner-Wohlfarth approximation and the interlayer coupling field of 200 Oe inferred from Fig. 1(a) was consistent with our estimates for the dipolar field induced by the 5-nm-thick patterned part of the polarizing layer. Both field and current-induced reversal occurred in a single well-defined step. The slope in Fig. 1(a) is caused by the continuous rotation of the free layer, due to the 40° misalignment of **H** with respect to the nanopillar easy axis. In our experience, large value of MR and single-step magnetic reversal consistent with single domain approximation are key to coherent current-induced precession of magnetic nanopillars. Hysteretic current-induced reversal at small H was replaced at $H\geq 500$ Oe by a peak caused by thermally activated reversible switching.[14] The peak disappeared at $H\geq 550$ Oe due to the transition to a dynamical state, as verified by the spectroscopic measurements described below.

III. MEASUREMENTS

Figure 2 shows the dependence of the measured power spectral density (PSD) on H. At $H=550$ Oe and $I<5$ mA, the spectra exhibited three harmonically related peaks caused by the clamshell precession. At $I>5$ mA, a spectral feature appeared at a frequency close to the second harmonic of the clamshell, consistent with the expected behavior of the OP mode. At $H>550$ Oe, this peak rapidly shifted to higher frequency. Simultaneously, the high-current part of the peak split from the lower part and eventually merged with the

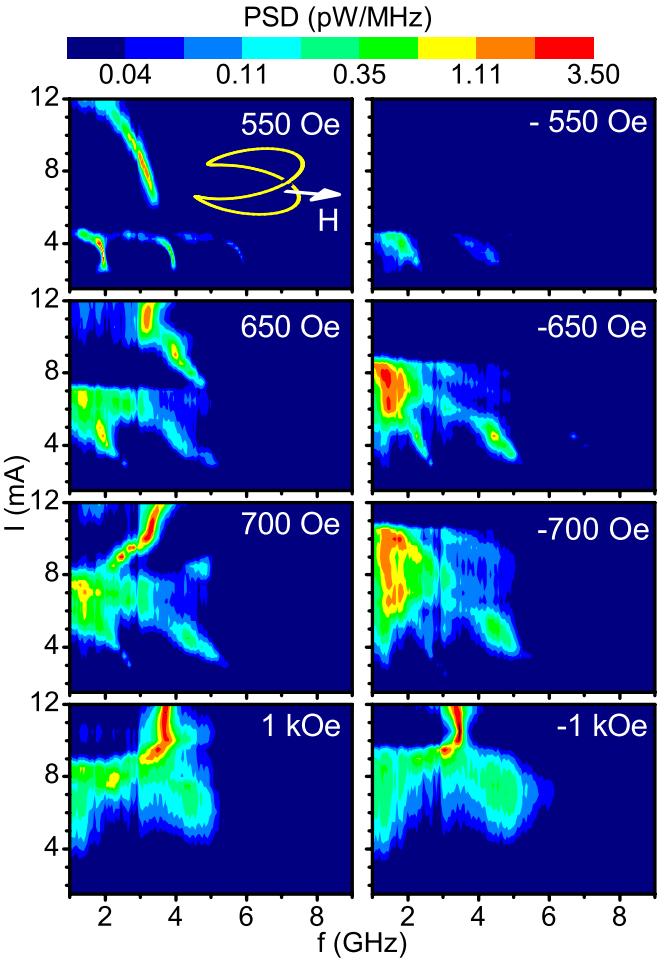

FIG. 2. (Color online) PSD vs frequency f and I, at the labeled values of H. Inset: clamshell trajectory of the magnetic moment, with **H** shown.

clamshell peaks ($H=650$ and 700 Oe data in Fig. 2).

The amplitude of precession producing these spectroscopic features can be determined by comparing the power emitted by the device to the largest possible power emitted by a hypothetical oscillation between antiparallel (AP) and parallel (P) configurations of the magnetic layers, $P_{\max}=I^2\Delta R^2 R_L/8(R+R_L)^2=37.7I^2$ pW for our sample, where I is in mA. Here, R is the average resistance during oscillation and $R_L=50$ Ω is the input impedance of the amplifier. This formula was obtained by considering an equivalent electric circuit consisting of a dc current source, oscillating resistance of the sample, and a load resistor $R_L=50$ Ω representing the input of the amplifier. The power generated by clamshell precession at $H=700$ Oe and $I=3.5$ mA is 137 pW, and by the OP mode at the same H and $I=10$ mA is 990 pW. Both values correspond to the precession angle exceeding 90°.

The high-current features can be caused by the spatially inhomogeneous dynamics rather than precession but such dynamical states are unlikely to produce microwave power approaching $P_{\max}$. Spatially inhomogeneous dynamical states are also more likely to play a significant role if the nanopillar is anomalously large, which is inconsistent with one of the largest values of MR reported for metallic devices. The qual-

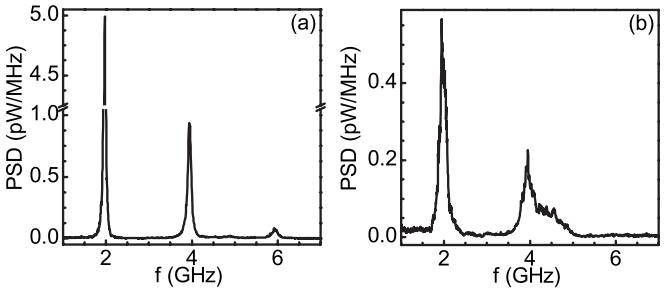

FIG. 3. Clamshell precession spectra acquired at $I=4$ mA, $\phi=48°$, (a) $H=600$ Oe and (b) $H=-600$ Oe.

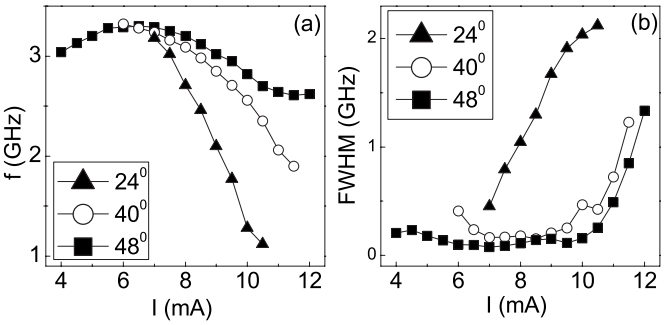

FIG. 4. Dependence of (a) frequency f and (b) FWHM of the OP peak on I for $\phi=48°$ (squares), $\phi=40°$ (open circles), and $\phi=24°$ (triangles).

ity of the device can also be characterized by analyzing the width of the precession peaks, which can be significantly broadened by the dynamical inhomogeneities.[15] The first harmonic of clamshell precession exhibits the smallest full width at half maximum (FWHM) of 30 MHz at $H=550$ Oe and $I=3.5$ mA, which is one of the smallest values reported for nanopillars at RT.

The clamshell peaks decrease in amplitude and broaden with increasing H, suggesting increasingly spatially inhomogeneous dynamics. In contrast, the intensity of the OP peak at $I=10$ mA increases from 0.86 pW/MHz at $H=550$ Oe to 2.5 pW/MHz at 1 kOe while the FWHM increases from 127 to 298 MHz. The spectra are asymmetric with respect to reversal of H (right panels in Fig. 2). The clamshell peaks are broader at $H<0$ than at $H>0$, and the OP mode is replaced by incoherent noise. The data became similar for $H=1$ and -1 kOe, exhibiting OP peak for both directions. Only a subset of our devices with extended polarizer exhibited coherent OP mode similar to the $H>0$ data in Fig. 2 while the rest of them, as well as all the devices with a nanopatterned polarizer, exhibited only broad spectral features similar to the $H<0$ data in Fig. 2. All devices exhibited a significant asymmetry with respect to the field reversal. Since the effects of field reversal have not been previously reported by other groups, we expect the asymmetry to be a common, although previously unnoticed, characteristic of current-induced dynamics. Asymmetry may also signify the inferior quality of our devices. However, the large MR exhibited by our samples, small width of the clamshell peaks for $H>0$, together with a robust signature of the OP mode, suggest that it is likely caused by the overall complexity of the current-induced dynamical states of nanopillars.

The asymmetry of dynamics with respect to the field reversal is also apparent for the clamshell precession at low current in Fig. 2, where the peaks at $H<0$ are consistently broader than at $H>0$. The mechanism for the broadening became evident when the angle ϕ was increased to 48°, as illustrated in Fig. 3 for two spectra acquired at the same I and opposite directions of field. The amplitude of the spectral peaks was larger at $H=600$ Oe than at $H=-600$ Oe while their FWHM was significantly smaller. The three precession harmonics in Fig. 3(a) can be accurately fitted with Lorentzians, yielding central frequencies of $f_1=1.97$ GHz, $f_2=3.95$ GHz, and $f_3=5.93$ GHz consistent with the first, second, and third harmonic, respectively, of precession at $f=1.975$ GHz. Fitting also yields FWHM of $\Delta f_1=37.7$ MHz, $\Delta f_2=90$ MHz, and $\Delta f_3=199$ MHz, and the total power under the peaks of $P_1=300$ pW, $P_2=136$ pW, and $P_3=23$ pW. In the macrospin approximation, the linewidths of the successive harmonics are expected to be proportional to the harmonic order if the broadening is dominated by thermal fluctuations of the magnetic moment transverse to the precessional trajectory, and to the square of the harmonic order if the broadening is dominated by fluctuations of the precession phase.[16] The ratio 1:2.4:5.3 for the FWHM of the harmonics in Fig. 3(a) indicates that both contributions are non-negligible, although the former dominates.

For $H=-600$ Oe, the first harmonic can be accurately fitted with a Lorentzian with parameters $f_1=1.97$ GHz, $\Delta f_1=166$ MHz, and $P_1=129$ pW. The second harmonic at $H<0$ exhibits a shoulder and is resolved by Lorentzian fitting into two separate peaks, with parameters $f_2=3.95$ GHz, $f'=4.43$ GHz, $\Delta f_2=238$ MHz, $\Delta f'=594$ MHz, $P_2=61$ pW, $P'=56$ pW. The shoulder was also present in $\phi=40°$ data but less distinct. The value of Δf_1 is more than half of Δf_2, indicating that the first harmonic may consist of two unresolved peaks. These results suggest that either an additional dynamical mode was excited simultaneously with precession or that the precession of the magnetic moment alternates between two different trajectories. The broadening and the reduced amplitude of the spectral peaks are direct consequences of the resulting reduction in precession coherence. The total emitted power is also reduced, indicating that the amplitude of the dynamics is suppressed by the additional dynamical state. It is presently unclear if this state is also responsible for the asymmetry of the OP dynamics.

We now focus on the analysis of the origin and properties of the high-current feature in spectra of Fig. 2. Out-of-plane precession is not the only possible explanation for this feature. Current-induced excitation of the polarizing layer F_2 can lead to microwave peaks, appearing above the onset current determined by the ratio of the volumes of F_2 and F_1.[6] However, the effective volume of the extended layer F_2 in our samples far exceeds that of F_1, and thus cannot explain the onset current that at 550 Oe is only 2.6 times larger than the onset of the clamshell precession. The nanopillar shape imperfections can also result in precession around a configuration intermediate between the AP and P states. However,

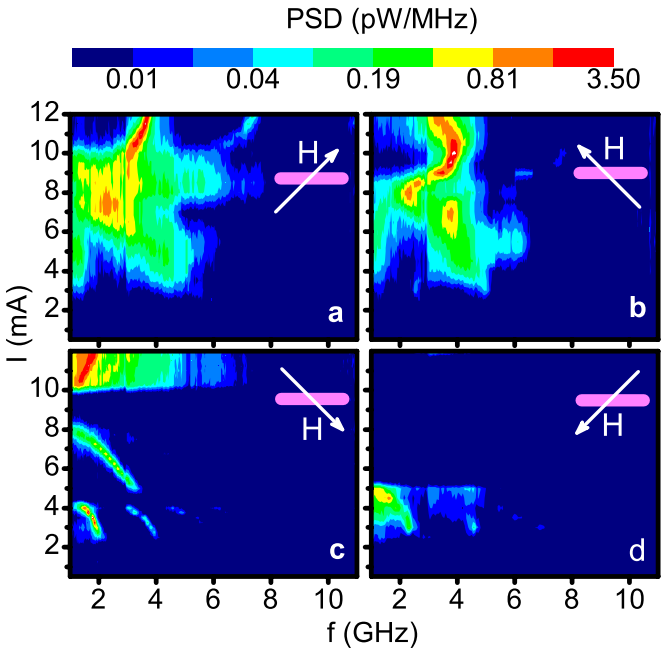

FIG. 5. (Color online) PSD for $|H|=900$ Oe tilted by 45° with respect to the sample plane, at $\phi=40°$. Insets are side-view schematics for the orientation of H with respect to the pillars, where in-plane direction of $H>0$ is to the right.

this intermediate state would quickly become unstable at increased H, contrary to the persistence of the observed spectral feature at large H in Fig. 2.

Further characterization of the dynamical states was performed by analyzing their response to both in-plane rotation and tilting of **H**. In-plane rotation of **H** affected the width of the OP peak and the dependence of its frequency on I (Fig. 4). At $\phi=48°$, the peak exhibited a blueshift up to 6.5 mA, above which it gradually redshifted. At smaller ϕ, the peak broadened, decreased in intensity, and redshifted. The correlation between the width of the OP peak and the dependence of its frequency on I is consistent with the effects of spatial magnetic inhomogeneity on precession. Specifically, the assumption of homogeneous dynamics (macrospin approximation) always entails blueshifting of the OP peak, which is caused by the increase in the demagnetizing field when the magnetic moment precesses further away from the sample plane with increasing I. Spatial inhomogeneity of dynamics results in reduced coherence of precession, leading to spectral broadening. It also causes a decrease in the total magnetic moment, reducing the demagnetizing field and thus the precession frequency.

The enhancement of precession coherence with increasing in-plane field angle with respect to the easy axis has been reported for clamshell precession in nanopillars by Thadani *et al.*[13] Their simulations showed that the enhancement is caused by the increased spatial homogeneity of the dynamics, although an alternative proposed explanation involved the effects of nonlinear frequency shift present even for homogeneous precession.[17] The coherence enhancement with increasing out-of-plane field angle has also been reported for current-induced precession in point contacts.[18] We observed enhancement of the clamshell and OP-mode coherence with increasing ϕ for all measured samples, suggesting that this effect is quite general.

Measurements with **H** tilted with respect to the sample plane provided additional information about the nature of the current-induced dynamical states. Figure 5 illustrates the results for 45° tilting angles both below and above the sample plane, at $H=900$ Oe. The perpendicular component of **H** was significantly smaller than the demagnetizing field of 9.4 kOe, resulting in estimated tilting of static $\mathbf{m}_1$ by only 5°. A sharp high-current feature associated with the OP mode appeared for both directions of **H** tilted above the film plane [panels (a) and (b)]. The $H>0$ data, panel (a), exhibit both the first and the second harmonics of the OP mode, consistent with the more coherent behaviors seen for $H>0$ in Fig. 2. In contrast, the high-current data for both directions of **H** tilted below the sample plane exhibit only incoherent low-frequency noise for $H>0$ and no detectable power for $H<0$. Besides the clamshell peaks, the $H>0$ data exhibit an additional feature between 4.5 and 5 mA, whose origin is presently unclear.

To qualitatively explain the effects of tilting on the OP mode in Fig. 5, we note that the OP trajectory is determined by the direction of **H** relative to the nanopillar easy axis. In our measurements, **H** was rotated clockwise with respect to the nanopillar easy axis, resulting in expected OP precession orbit located below the plane. In addition, the OP trajectory tends to oppose the effective field determined by a combination of H and the demagnetizing field. Tilting **H** below the film plane can then favor precession above the plane but not the OP dynamics below the plane. This qualitative analysis is supported by the simulations described below.

IV. SIMULATIONS

To clarify the effects of rotation/tilting of **H** on the OP dynamics and the mechanism of the asymmetry with respect to the field reversal, we performed micromagnetic simulations with OOMMF open source software.[19] To the best of our knowledge, even advanced published simulations were not able to quantitatively reproduce the spectroscopic measurements.[2,4,20] Therefore, the goal of our simulations was set to identify the origins of the observed trends, rather than quantitatively fit the experiment.

The simulations included the current-induced ST and Oersted-field effects but neglected thermal fluctuations. To account for the dipolar field of the partially patterned polarizer F_2, a field $H_d=200$ Oe was subtracted from the in-plane component of **H**. The cell size was $4\times4\times5$ nm^3 and the nanopillar dimensions $104\times52\times5$ nm^3. We performed several calculations with the cell size reduced to $2\times2\times5$ nm^3, yielding similar results. Standard Py magnetic and spin-dependent electronic parameters were used: current polarization $p=0.7$,[21] Py exchange stiffness $A=1.3\times10^{-6}$ erg/cm,[19] and the ratio $\Lambda=1.3$ of the ST magnitudes for a small defelction from the AP and the P states, respectively.[22] Saturation magnetization $M=750$ emu/cm^3 of Py was determined by magnetometry of a Py(5) film prepared under the same conditions as the nanopillar. The values of Gilbert damping parameter in Py nanopillars determined

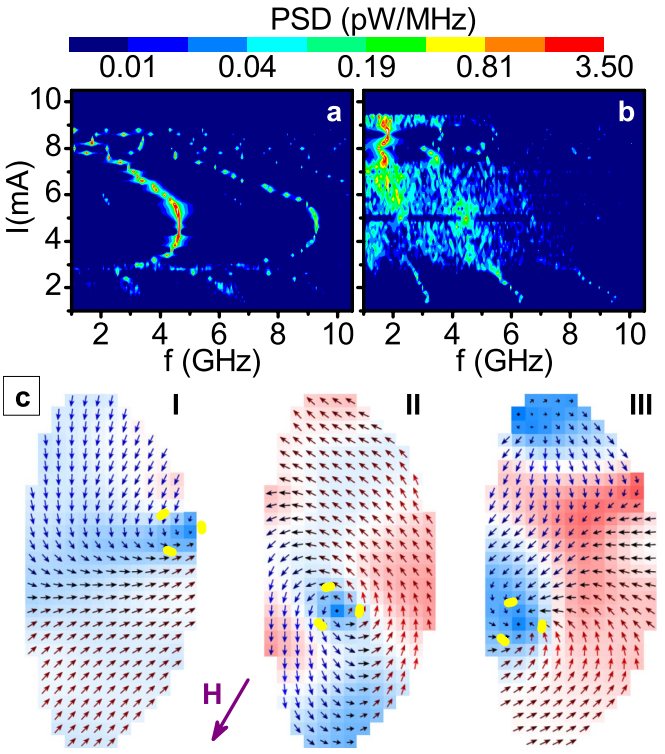

FIG. 6. (Color online) (a) Calculated PSD for $H=650$ Oe. (b) same as (a), for $H=-650$ Oe. (c) instantaneous magnetization distribution for $H=-650$ Oe, $I=6$ mA, captured in the I-II-III sequence with a 100 ps interval, showing the nucleation, propagation, and annihilation of a vortex; the motion of its core is marked with yellow dots. The intensity of blue(red) reflects the out-of-plane component of the magnetization above(below) the plane. Arrow shows the direction of H.

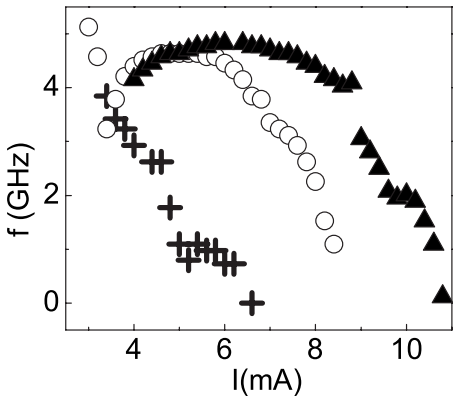

FIG. 7. Simulated frequency of the OP peak vs I for $\phi=48°$ (triangles), $\phi=40°$ (open circles), and $\phi=24°$ (crosses), at $H=650$ Oe.

by different techniques can vary between 0.01 and 0.03.[16,23–25] We adjusted the value of α in our simulations so that the simulated precession onset current matched with the value $I_C=1.4$ mA determined from the step in dV/dI at $H>500$ Oe caused by the onset of current-induced dynamics,[14] yielding $\alpha=0.03$. The value of I_C determined from the direct spectroscopic measurements is less precise since the width of the precession peaks diverges near the precession onset.[16] The value of α and consequently I_C generally depends on T, which was neglected in our simulations. However, variable-temperature measurements indicate that this dependence is small for unoxidized Py.[11,12,14]

The spectra were calculated from the simulated time-dependent magnetization distribution of the nanopillar. The calculated time-dependent resistance was $R(t)=R_0+\Delta R(t)$, where $R_0=(R_P+R_{AP})/2$ and $\Delta R(t)=(R_P-R_{AP})\langle \mathbf{s_1}\cdot\mathbf{s_2}\rangle/2$. Here, $\mathbf{s}_1(t),\mathbf{s}_2(t)$ are the local normalized magnetizations of F_1 and F_2, and $\langle\ \rangle$ denotes averaging over the simulation grid. The ac voltage on the input of the amplifier $V(t)=\frac{I\Delta R(t)}{1+R_0/50\ \Omega}$ was calculated by assuming that a constant current I was split between a $R_L=50\ \Omega$ load and a resistor $R(t)$ representing the sample. Fast Fourier transform (FFT) of $V(t)$ over a period of $T=16.4$ ns with a 1 ps step was performed after relaxation for 10 ns. The power spectral density was determined by $\mathrm{PSD}(f)=2V^2(f)/(50\ \Omega\Delta f)$, where $\Delta f=1/T$, and a factor of 2 accounts for the negative-f contribution to the FFT.

The calculations of the effects of field rotation and tilting captured the key features of our measurements, as described below. However, the asymmetry of the spectra could not be reproduced for elliptical nanopillars with any reasonable values of the magnetic parameters, distribution of current through the nanopillar cross section, or Oersted field of the current through the pillar and the leads. Rather, the asymmetry appeared in simulations once the defects of the sample shape were introduced simultaneously with the Oersted field of the current.

SEM imaging of our nanopillars shows that local edge roughness is the most likely type of shape defects. However, the overall consequences of defects can be also analyzed by

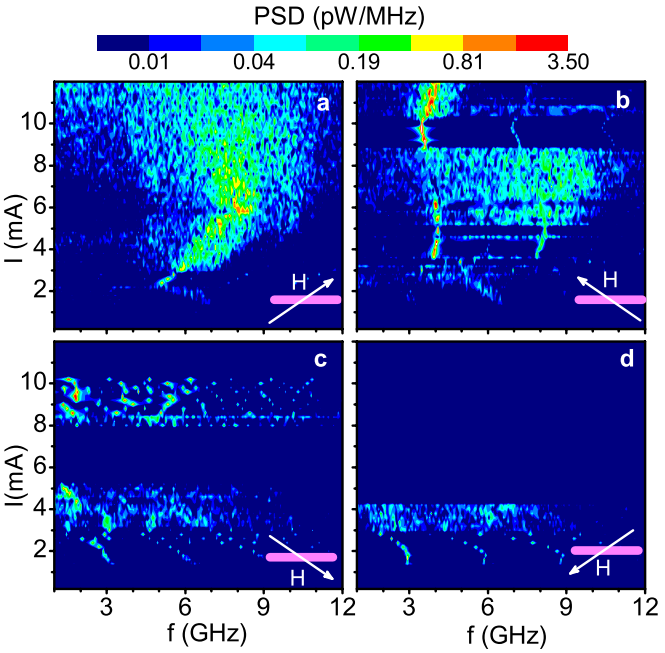

FIG. 8. (Color online) Simulated PSD for $|H|=900$ Oe tilted by 45° with respect to the sample plane, at $\phi=40°$. Insets are side-view schematics for the orientation of H with respect to the pillars. $H>0$ is directed to the right.

introducing smooth shape distortions. Here, we describe simulations for a nanopillar approximated by two semiellipses with minor semiaxes of 34 and 18 nm, and a common major axis of 104 nm. Coherent OP precession was obtained at $H>0$ [Fig. 6(a)] but was suppressed at $H<0$ [Fig. 6(b)]. Instead of the OP mode, the dynamics involved segments of clamshell precession with a significantly spatially inhomogeneous magnetic configuration, which were terminated by the entrance and propagation through the nanopillar of dynamical vortices. This dynamical state lacked periodicity, resulting in a broad spectral feature similar to that in our $H=-600$ Oe and $H=-650$ Oe data in Fig. 2, and the broad high-current spectroscopic features seen by others.[6]

Vortex nucleation caused by local crystalline anisotropy was also suggested[15] as a mechanism for the observed spectral broadening in cobalt.[5] In our simulations with the selected nanopillar shape asymmetry, the vortices usually nucleated at the right upper edge of the nanopillar, and annihilated at the lower left edge [Fig. 6(c)]. The chirality of the vortices coincided with the direction of the Oersted field, indicating that the asymmetry of spectra is caused by the enhancement or suppression of vortex nucleation due to the interplay of sample geometry and the effect of Oersted field.

Simulations were also performed for different orientations of **H**. At small angle between the in-plane **H** and the nanopillar easy axis, the OP mode involved significant dynamical inhomogeneity of the magnetic distribution, resulting in the redshift of precession frequency with increasing I, as illustrated with crosses for $\phi=24°$ in Fig. 7. Rotation of **H** in the film plane away from the nanopillar easy axis resulted in a more homogeneous magnetic configuration and a blueshift of the OP mode over an increasing range of I, as shown in Fig. 7 for $\phi=40°$ (circles) and $\phi=48°$ (triangles). These results are consistent with our analysis of data in Fig. 4.

Simulations with **H** tilted above the sample plane yielded OP precession below the plane both for $H>0$ [Fig. 8(a)] and $H<0$ [Fig. 8(b)]. For $H>0$, the precession resulted in a broad spectral feature due to the dynamical inhomogeneities. However, the evolution of the magnetic configuration with time was consistent with a robust OP mode. The OP precession at $H<0$ became possible because the vortex nucleation was suppressed by tilted **H**. Further analysis is needed to better understand the mechanisms of this suppression.

With **H** tilted below the plane, the simulations showed suppressed OP precession both at $H>0$ and $H<0$ [Figs. 8(c) and 8(d)]. The broad spectral features at $H>0$ were caused by complex inhomogeneous dynamics including multiple vortices nucleating and propagating through the nanopillar. For $H<0$, the simulated dynamics were completely suppressed at $I>4$ mA. These simulated effects of field tilting are in excellent agreement with the data of Fig. 5.

V. SUMMARY

We have performed spectroscopic measurements of magnetic dynamics in magnetic nanopillars with an extended polarizing magnetic layer. Our measurements yielded a high-current spectral feature whose dependence on the direction of field **H** is consistent with the OP precession mode. We verified the key properties of the OP precession: (i) its frequency is approximately twice the frequency of the clamshell precession near the crossover, (ii) rotation of the magnetic field in the film plane away from the nanopillar easy axis results in narrowing of the precession peak and simultaneously increasing blueshift of the OP mode, and (iii) tilting the magnetic field below the sample plane, in the direction of the OP orbit, results in suppression of this mode.

The dynamics exhibited a significant asymmetry with respect to reversal of **H**. Simulations suggest that the asymmetry is caused by the combined effects of the sample shape imperfections and Oersted field of the current, resulting in vortex nucleation only for one direction of the field. We modeled the imperfections of the nanopillar by an asymmetric semielliptical shape, resulting in general agreement between the simulation results and our measurements.

Simulations could not reproduce several features of the data. First, the simulated OP peak did not exhibit the rapid shift and splitting with increasing H seen in data. Second, despite a significant asymmetry of the calculated spectra, simulations did not reproduce the region at $I>5$ mA, where a sharp OP peak was present for $H=500$ Oe but no dynamical features appeared at $H=-550$ Oe. The simulations also indicated that the OP mode should exhibit multiple spectral harmonics while only one or two harmonics could be seen in data, regardless of the large amplitude of precession established from the analysis of the emitted microwave power. These features suggest that the complex magnetic dynamics of the nanopillar is in subtle ways affected by its properties such as details of the shape, local anisotropy variations, interface roughness, and current distribution. It is also possible that the micromagnetic simulations do not adequately describe highly excited states of nanomagnets subjected to large spin torques.

Our results show that spatially inhomogeneous dynamics and vortices play a more significant role than was previously assumed. The Oersted field of the current favors the formation of vortices but their static configuration is not stable in our nanopillars even at large currents.[26] However, dynamical nucleation of vortices and their propagation through nanopillar over subnanosecond time scale becomes possible due to shape defects providing the nucleation sites. Our spectroscopic data also correlate with time-resolved measurements of current-induced dynamics,[27] which showed that sufficiently large (110 nm$\times$150 nm) nanopillars reverse through intermediate vortex states. Our results suggest that even for smaller nanopillars, the reversal path may be determined by a combination of detailed shape, values of current and its distribution. It is possible that precise shape engineering in magnetic nanodevices may facilitate fast nanopillar switching through dynamical vortex formation, without compromising their stability in the absence of current.

ACKNOWLEDGMENTS

This work was supported by NSF under Contract No. DMR-0747609 and by the Cottrell Scholarship from the Research Corporation.

[1] J. Slonczewski, J. Magn. Magn. Mater. **159**, L1 (1996).
[2] D. V. Berkov and J. Miltat, J. Magn. Magn. Mater. **320**, 1238 (2008).
[3] Z. Li and S. Zhang, Phys. Rev. B **68**, 024404 (2003).
[4] D. V. Berkov and N. L. Gorn, Phys. Rev. B **72**, 094401 (2005).
[5] S. I. Kiselev, J. C. Sankey, I. N. Krivorotov, N. C. Emley, R. J. Schoelkopf, R. A. Buhrman, and D. C. Ralph, Nature (London) **425**, 380 (2003).
[6] S. I. Kiselev, J. C. Sankey, I. N. Krivorotov, N. C. Emley, A. G. F. Garcia, R. A. Buhrman, and D. C. Ralph, Phys. Rev. B **72**, 064430 (2005).
[7] O. Boulle, V. Cros, J. Grollier, L. G. Pereira, C. Deranlot, F. Petroff, G. Faini, J. Barnas, and A. Fert, Nat. Phys. **3**, 492 (2007); Phys. Rev. B **77**, 174403 (2008).
[8] S. Urazhdin, Phys. Rev. B **78**, 060405(R) (2008).
[9] W. L. Lim, A. Higgins, and S. Urazhdin, Appl. Phys. Lett. **92**, 172501 (2008).
[10] W. L. Lim, A. Higgins, and S. Urazhdin, arXiv:0810.0863 (unpublished).
[11] O. Ozatay, P. G. Gowtham, K. W. Tan, J. C. Read, K. A. Mkhoyan, M. G. Thomas, G. D. Fuchs, P. M. Braganca, E. M. Ryan, K. V. Thadani, J. Silcox, D. C. Ralph, and R. A. Buhrman, Nature Mater. **7**, 567 (2008).
[12] S. Urazhdin and P. Tabor, J. Appl. Phys. **105**, 066105 (2009).
[13] K. V. Thadani, G. Finocchio, Z.-P. Li, O. Ozatay, J. C. Sankey, I. N. Krivorotov, Y.-T. Cui, R. A. Buhrman, and D. C. Ralph, Phys. Rev. B **78**, 024409 (2008).
[14] S. Urazhdin, N. O. Birge, W. P. Pratt, Jr., and J. Bass, Phys. Rev. Lett. **91**, 146803 (2003).
[15] K. J. Lee, A. Deac, O. Redon, J. P. Noziers, and B. Dieny, Nature Mater. **3**, 877 (2004).
[16] J. C. Sankey, I. N. Krivorotov, S. I. Kiselev, P. M. Braganca, N. C. Emley, R. A. Buhrman, and D. C. Ralph, Phys. Rev. B **72**, 224427 (2005).
[17] J.-V. Kim, V. Tiberkevich, and A. N. Slavin, Phys. Rev. Lett. **100**, 017207 (2008).
[18] W. H. Rippard, M. R. Pufall, and S. E. Russek, Phys. Rev. B **74**, 224409 (2006).
[19] M. J. Donahue and D. G. Porter, *OOMMF User's Guide* (NIST, Gaithersburg, MD, 1999).
[20] I. N. Krivorotov, D. V. Berkov, N. L. Gorn, N. C. Emley, J. C. Sankey, D. C. Ralph, and R. A. Buhrman, Phys. Rev. B **76**, 024418 (2007).
[21] J. Bass and W. P. Pratt, Jr., J. Phys.: Condens. Matter **19**, 183201 (2007).
[22] S. Urazhdin, N. O. Birge, W. P. Pratt, Jr., and J. Bass, Appl. Phys. Lett. **84**, 1516 (2004).
[23] N. C. Emley, I. N. Krivorotov, O. Ozatay, A. G. F. Garcia, J. C. Sankey, D. C. Ralph, and R. A. Buhrman, Phys. Rev. Lett. **96**, 247204 (2006).
[24] J. C. Sankey, P. M. Braganca, A. G. F. Garcia, I. N. Krivorotov, R. A. Buhrman, and D. C. Ralph, Phys. Rev. Lett. **96**, 227601 (2006).
[25] G. D. Fuchs, J. C. Sankey, V. S. Pribiag, L. Qian, P. M. Braganca, A. G. F. Garcia, E. M. Ryan, Zhi-Pan Li, O. Ozatay, D. C. Ralph, and R. A. Buhrman, Appl. Phys. Lett. **86**, 152509 (2005).
[26] S. Urazhdin, C. L. Chien, K. Y. Guslienko, and L. S. Novozhilova, Phys. Rev. B **73**, 054416 (2006).
[27] J. P. Strachan, V. Chembrolu, Y. Acremann, X. W. Yu, A. A. Tulapurkar, T. Tyliszczak, J. A. Katine, M. J. Carey, M. R. Scheinfein, H. C. Siegmann, and J. Stohr, Phys. Rev. Lett. **100**, 247201 (2008).